

Pericardial Adipose Tissue Regulates Granulopoiesis, Fibrosis, and Cardiac Function After Myocardial Infarction

BACKGROUND: The pericardial adipose tissue (AT) contains a high density of lymphoid clusters. It is unknown whether these clusters play a role in post-myocardial infarction (MI) inflammatory responses and cardiac outcome.

METHODS: Lymphoid clusters were examined in epicardial AT of humans with or without coronary artery disease. Murine pericardial lymphoid clusters were visualized in mice subjected to coronary artery ligation. To study the relevance of pericardial clusters during inflammatory responses after MI, we surgically removed the pericardial AT and performed B-cell depletion and granulocyte-macrophage colony-stimulating factor blockade. Leukocytes in murine hearts, pericardial AT, spleen, mediastinal lymph nodes, and bone marrow were quantified by flow cytometry. Cannabinoid receptor CB2 (CB2^{-/-}) mice were used as a model for enhanced B-cell responses. The effect of impaired dendritic cell (DC) trafficking on pericardial AT inflammatory responses was tested in CCR7^{-/-} mice subjected to MI. Cardiac fibrosis and ventricular function were assessed by histology and echocardiography.

RESULTS: We identified larger B-cell clusters in epicardial AT of human patients with coronary artery disease in comparison with controls without coronary artery disease. Infarcted mice also had larger pericardial clusters and 3-fold upregulated numbers of granulocyte-macrophage colony-stimulating factor-producing B cells within pericardial AT, but not spleen or lymph nodes. This was associated with higher DC and T-cell counts in pericardial AT, which outnumbered DCs and T cells in lymph nodes. Analysis of DC maturation markers, tracking experiments with fluorescently labeled cells, and use of CCR7-deficient mice suggested that activated DCs migrate from infarcts into pericardial AT via CCR7. B-cell depletion or granulocyte-macrophage colony-stimulating factor neutralization inhibited DC and T-cell expansion within pericardial AT, and translated into reduced bone marrow granulopoiesis and cardiac neutrophil infiltration 3 days after MI. The relevance of the pericardial AT in mediating all these effects was confirmed by removal of pericardial AT and ex vivo coculture with pericardial AT and granulocyte progenitors. Finally, enhanced fibrosis and worsened ejection fraction in CB2^{-/-} mice were limited by pericardial AT removal.

CONCLUSIONS: Our findings unveil a new mechanism by which the pericardial AT coordinates immune cell activation, granulopoiesis, and outcome after MI.

Michael Horckmans, PhD
Mariaelvy Bianchini, MSc
Donato Santovito, MD
Remco T.A. Megens, PhD
Jean-Yves Springael, PhD
Irene Negri, MSc
Michele Vacca, MD
Marco Di Eusanio, MD
Antonio Moschetta, MD
Christian Weber, MD
Johan Duchene, PhD
Sabine Steffens, PhD

Key Words: B-lymphocytes ■ dendritic cells ■ granulocyte-macrophage colony-stimulating factor ■ hematopoietic stem cells ■ lymphoid tissue ■ stem cells

Sources of Funding, see page 959

© 2017 American Heart Association, Inc.

<http://circ.ahajournals.org>

Clinical Perspective

What Is New?

- The pericardial adipose tissue contains a high density of lymphoid clusters that serve as secondary lymphoid organs in which B cells, dendritic cells, and T cells expand in response to myocardial infarction.
- Local release of cytokines and growth factors within the pericardial adipose tissue, as well as systemically released factors, promote immune cell proliferation and emergency granulopoiesis after myocardial infarction.
- It is most important to note that the pericardial adipose tissue critically regulates cardiac fibrosis and preservation of ventricular function in response to myocardial infarction.

What Are the Clinical Implications?

- Our preclinical data suggest that the pericardial adipose tissue is a central compartment for innate and adaptive immune responses that regulate post-myocardial infarction healing.
- Changes in pericardial and epicardial adipose tissue inflammatory milieu might affect the clinical outcomes in patients with myocardial infarction, opening a new avenue for searching for more tailored therapies to improve cardiac remodeling and prevent heart failure after myocardial infarction.

Cardiomyocyte necrosis in response to myocardial infarction (MI) activates an immediate immune response to promote cardiac repair. Whereas the role of innate immune cells, in particular monocytes and neutrophils, in this inflammatory process has been extensively studied, the role of adaptive immune cells such as B and T lymphocytes during the early immune response after MI is less clear. Zougari et al¹ demonstrated that B cells contribute to myocardial injury and unfavorable remodeling by inducing the release of Ly6C⁺ monocytes from the bone marrow via secretion of CCL7. This study essentially focused on the role of B cells on collagen deposition and impaired heart function 14 days after MI.

As opposed to experimental data reporting a peak of lymphocytes infiltrating murine hearts around day 5 to 7 post-MI, analysis of transcortical gradients from patients with MI suggests an early recruitment of T and B lymphocytes from peripheral blood into the myocardium within 90 minutes of reperfusion.² This is reflected by the loss of circulating lymphocytes and associated with a poor prognosis.² However, because myocardium and epicardial adipose tissue (AT) share the same microcirculation in humans,³ it is conceivable that lymphocytes are recruited in part in the epicardial AT.

In support of a possible lymphocyte recruitment into AT, it was recently described that B and T cells are retained in so-called fat-associated lymphoid clusters (FALCs) in the peritoneal and pleural cavity of mice, which are a type of lymphoid tissue present in visceral fat.⁴ It is remarkable that the pericardium contains the highest density of these FALCs in the pleural cavity,⁴ suggesting a possible relevance as a secondary lymphoid organ in response to cardiac injury.

The inflammatory process after MI is accompanied by an increase of circulating cytokines that might affect FALC formation and function. However, whether pericardial FALCs and immune cell activation in these clusters might play a role during early inflammatory responses after ischemic cardiac injury is unknown. We therefore addressed MI-induced inflammatory responses in pericardial AT and activation of lymphocytes and dendritic cells (DCs) within FALCs, and whether this might affect innate immune cells during acute inflammatory responses and cardiac healing and function after MI.

METHODS

Detailed methods are available in the [online-only Data Supplement](#). Requests by researchers to access the data, analytic methods, and study materials for the purposes of reproducing the results or replicating procedures can be made to the corresponding author who manages the information.

Animal Experiments

Female 10- to 12-week-old C57BL/6J wild-type (WT), CB2^{-/-},⁵ and CCR7^{-/-6} mice were used in this study. MI was induced by permanent ligation of the left anterior descending coronary artery (LAD). Mice were anesthetized, intubated, and ventilated with a MiniVent mouse ventilator (Harvard Apparatus). A left thoracotomy was performed in the fourth left intercostal space, and the pericardium was carefully incised to maintain the integrity of the pericardial AT. MI was induced by permanent ligation of the LAD proximal to its bifurcation from the main stem, and the chest wall and skin subsequently were closed. Postoperative analgesia (buprenorphine, 0.1 mg/kg) was given for the first 12 hours after surgery. In some experiments, mice received intramyocardial injections of DCs labeled with cell tracker SP-DiOC18 (Molecular Probes) in the ischemic LAD territory. B-cell depletion was performed by intraperitoneal injection of a mixture of monoclonal antibodies at 150 µg/mouse each, as previously described⁷: rat anti-mouse CD19 (clone 1D3), rat anti-mouse B220 (clone RA36B2), and mouse anti-mouse CD22 (clone CY34). After 48 hours, mice were injected intraperitoneally with a secondary antibody mouse anti-rat kappa (clone TIB216) at 150 µg/mouse before LAD ligation.⁷ Control mice received corresponding isotype intraperitoneal injections. Anti-granulocyte-macrophage colony-stimulating factor (GM-CSF) blocking antibody (100 µg/mouse) or vehicle (saline) was injected intraperitoneally 15 minutes before, and 1 and 2 days after LAD ligation, as

well.⁸ Splenectomy was performed 7 days before LAD ligation. In selective experiments, pericardial AT ($\approx 80\%$) was removed before LAD ligation. All animal experiments were approved by the local ethical committee (District of Upper Bavaria, Germany).

Human Specimen

White male patients undergoing cardiac surgery were recruited at the Department of Cardiothoracic Surgery, Policlinico S. Orsola-Malpighi, University of Bologna. Patients in the control group ($n=5$) underwent elective cardiac valve surgery, and patients with coronary artery disease (CAD) ($n=6$) underwent elective coronary artery bypass graft surgery. In the control group, only patients with no history of CAD and cerebrovascular disease, and no instrumental evidence of CAD and carotid atherosclerosis, were recruited. At the time of recruitment, none of the control subjects included in the study underwent pharmacological therapy, except for antihypertensive drugs (including β -blockers). During the surgical procedures, epicardial AT and subcutaneous AT were collected for histological characterization. Adipose biopsy samples were obtained before the initiation of cardiopulmonary bypass from areas that had not previously been injured mechanically or cauterized. Epicardial AT was taken from the anterior surface of the heart near the anterior descending coronary artery or, alternatively, along the atrioventricular groove in proximity of the right coronary artery. Subcutaneous AT was taken from the subcutaneous fat on the sternum. Tissues were immediately fixed in formalin for histology. The human study protocol was approved by the Azienda Sanitaria Locale of Bari and the Policlinico S. Orsola-Malpighi (University Hospital) of Bologna Ethics Committees. All patients gave their informed consent for the use of clinical data and blood samples for scientific research purposes connected to this project. The principles of the Declaration of Helsinki were followed.

Statistics

Statistical analyses were performed with Prism (version 6; GraphPad). Unless noted differently, data are expressed as mean \pm SEM. Comparison between 2 groups was analyzed by the Student *t* test, applying the Welch correction when appropriate. To test significance in comparisons involving ≥ 3 groups, we applied the 1-way or 2-way ANOVA depending on the number of factors involved, and followed by the Bonferroni post hoc test for assessing pairwise differences among groups. For the comparison of stem cell distribution within the different cell cycle phases, we applied the χ^2 test. A 2-tailed $P < 0.05$ was deemed statistically significant.

RESULTS

MI Induces Proliferation of B Cells Within Pericardial AT

To clarify whether MI induces B-cell expansion within pericardial AT, we subjected WT mice to MI and performed flow-cytometric analysis of heart and AT. We detected only a few B cells in murine hearts at baseline

without significant increases 1 to 7 days after MI, but ≈ 100 -fold higher numbers in pericardial AT ($\approx 1 \times 10^6/g$ in hearts versus $\approx 1 \times 10^8/g$ in AT, baseline), which further increased ≈ 3 -fold in AT after 3 days of MI (Figure 1A through 1C). This time point represents the peak of B-cell accumulation in the pericardial AT, with subsequent decrease until day 7 (Figure 1C).

The cannabinoid receptor CB2, which is abundantly expressed on B cells,⁹ is required for the retention of immature B cells in the bone marrow within the sinusoidal niche and is thought to play an important role in B-cell repertoire formation.¹⁰ We therefore thought to use CB2-deficient mice as an additional model for studying the sequential role of B cells during post-MI inflammatory responses. We used only females in this study, because of a larger amount of pericardial AT (Figure 1A through 1C in the online-only Data Supplement). CB2^{-/-} mice had elevated B-cell counts in hearts and pericardial AT in comparison with WT mice (Figure 1A through 1C) and larger pericardial clusters, as shown by immune fluorescence (Figure 1D in the online-only Data Supplement) and 2-photon laser-scanning microscopy (Figure 1D). In human epicardial AT from patients with CAD, we also found B-cell clusters, which were larger in size than control epicardial AT samples from patients without CAD (Figure 1E, Figure 1D in the online-only Data Supplement). B-cell clusters were undetectable in subcutaneous AT from patients with CAD (Figure 1E in the online-only Data Supplement).

To investigate the underlying mechanism of B-cell expansion within pericardial AT in response to MI, we first assessed bone marrow lymphopoiesis, which did not reveal differences between WT and CB2^{-/-} mice. We found overall lower numbers of lymphoid progenitors 1 day after MI in comparison with noninfarcted mice irrespective of the genotype (Figure 1F in the online-only Data Supplement). We asked whether lymphocytes are mobilized from the spleen in response to MI. However, splenectomy only partially reduced B-cell numbers infiltrating the AT, albeit plasma chemokines involved in lymphocyte recruitment (CXCL5, CXCL10, CCL2) were detectable 1 day post-MI and significantly higher in CB2^{-/-} in comparison with WT mice (Figure 1G and 1H in the online-only Data Supplement). Another explanation for lymphocyte expansion post-MI might be proliferation, driven by proinflammatory plasma cytokines (tumor necrosis factor- α , interleukin [IL]-9, and IL-13), which were detectable in WT mice 1 day after MI and significantly higher in CB2^{-/-} mice (Figure 1I in the online-only Data Supplement). Indeed, we confirmed higher numbers of proliferating B cells in the pericardial AT of WT mice, and even higher numbers of B cells in G1 and G2/S/M phase in CB2^{-/-} than in WT mice, whereas the percentage in G0 decreased (Figure 1F).

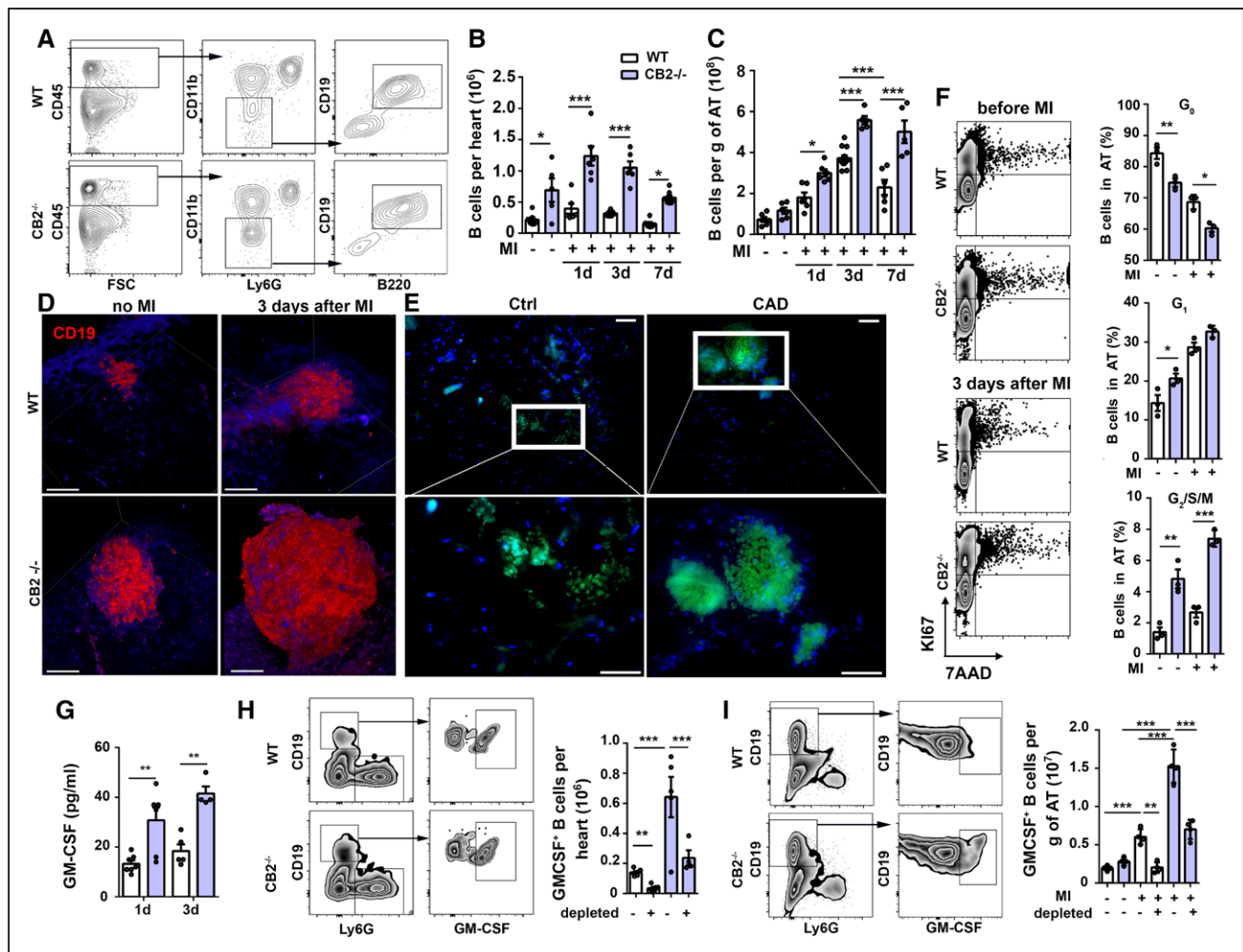


Figure 1. Myocardial infarction promotes B-cell proliferation in pericardial adipose tissue.

A, Gating strategy for flow-cytometric quantification of murine cardiac B cells. **B**, CD19⁺ B220⁺ B cells in hearts of WT and CB2^{-/-} mice at steady state or after 1, 3, and 7 days post-MI (n=6). **C**, B cells in pericardial adipose tissue (AT) at steady state or 1, 3, and 7 days post-MI (n=6). **D**, Three-dimensional TPLSM reconstruction of CD19 (red) and autofluorescent components (collagen, adipocytes; blue) in pericardial AT of WT and CB2^{-/-} mice. Scale bars represent 100 μm. **E**, Immunofluorescence staining on paraffin sections of CD19⁺ B cells (green) and nuclei (blue) in human epicardial AT of patients with or without coronary artery disease (CAD). **F**, Representative dot plots with quadrants to identify cells in G₀ (Lower Left), G₁ (Upper Left), and G₂/S/M (Upper Right) cell cycle phases. Proliferating B cells in pericardial AT from WT and CB2^{-/-} mice at steady state or 3 days post-MI (n=3). **G**, Plasma levels of GM-CSF 1 and 3 days after MI (n=4–6). **H**, Representative FACS plots (Left) and quantification (Right) of cardiac GM-CSF⁺ B cells 3 days after MI, with or without B-cell depletion. **I**, Representative FACS plots (Left) and quantification (Right) of GM-CSF⁺ B cells in pericardial AT 3 days after MI, with or without B cell depletion (n=4–6). Results are pooled from at least 3 independent experiments. Mean values±SEM are shown. *P<0.05. **P<0.01. ***P<0.001. Ctrl indicates control; FACS, fluorescence-activated cell sorting; FSC, forward scatter; GM-CSF, granulocyte-macrophage colony-stimulating factor; MI, myocardial infarction; TPLSM, 2-photon laser-scanning microscopy; and WT, wild type.

GM-CSF–Producing B Cells Expand in Pericardial AT After MI

The multiplex immunoassay of murine plasma after MI further revealed increased plasma levels of GM-CSF in CB2^{-/-} in comparison with WT mice (Figure 1G). Among various cell types, such as macrophages, fibroblasts, and endothelial cells, producing GM-CSF, B cells also represent a relevant source.¹¹ We asked whether GM-CSF–producing B cells expand during early inflamma-

tory responses post-MI. Flow-cytometric analysis confirmed the presence of GM-CSF⁺ B cells in infarcted hearts and pericardial AT of WT mice 3 days after MI (Figure 1H and 1I). It is striking that their numbers were much higher in CB2^{-/-} mice. To validate our findings, we systemically depleted B cells with an antibody cocktail (Figure II in the online-only Data Supplement), which significantly reduced GM-CSF⁺ B-cell counts in infarcted hearts and pericardial AT (Figure 1H and 1I). To assess the distribution of GM-CSF–producing B cells

and preferential expansion sites in response to MI, we compared their numbers in various lymphoid organs. We found the highest amounts of GM-CSF⁺ B cells in the spleen (Figure IIIA through IIIC in the online-only Data Supplement). In proximity to the heart, most GM-CSF⁺ B cells were localized in pericardial AT, but only at low numbers within mediastinal lymph nodes (Figure III in the online-only Data Supplement). After MI, GM-CSF⁺ B cells expanded only in pericardial AT, not in mediastinal lymph nodes or spleen (Figure IIIA through IIIC in the online-only Data Supplement). FALCs were originally described in the peritoneal cavity.⁴ Given that MI induces an acute increase of inflammatory cytokines in the circulation, we may speculate that MI also supports an expansion of B cells and FALCs in other AT beds. Hence, we performed flow cytometry analysis of visceral AT from infarcted mice. Besides an overall small number of leukocytes in visceral in comparison with pericardial AT, we observed that B cells are only a minor population among all visceral AT leukocytes (Figure IIID through IIIF in the online-only Data Supplement), indicating a specific activation of B cells in pericardial AT in response to MI.

B Cells Promote DC Accumulation in the Ischemic Myocardium and Pericardial AT

To address a possible role for GM-CSF⁺ B cells in inflammatory responses post-MI, we first asked whether B-cell depletion affects other cellular key players involved in this process. In agreement with previously published data,¹ we found significantly lower cardiac monocyte counts in B-cell-depleted WT mice 3 days after MI (Figure 2A and 2B). It is noteworthy that monocyte counts in infarcted hearts of CB2^{-/-} mice were similar to the WT group, whereas cardiac macrophage counts were significantly higher in CB2^{-/-} mice (Figure 2C). B-cell depletion blunted cardiac macrophage increase in CB2^{-/-} mice, suggesting that B cells not only promote monocyte recruitment, but also possibly local proliferation in the myocardium (Figure 2C).

Deficiency of CB2 was accompanied by higher numbers of cardiac DCs evidenced 3 days after MI, whereas B-cell depletion reduced the number of DCs in both WT and CB2^{-/-} mice (Figure 2D). Even higher DC counts were detected in pericardial AT after MI, in particular in CB2^{-/-} mice (Figure 2E). Analysis of the tissue distri-

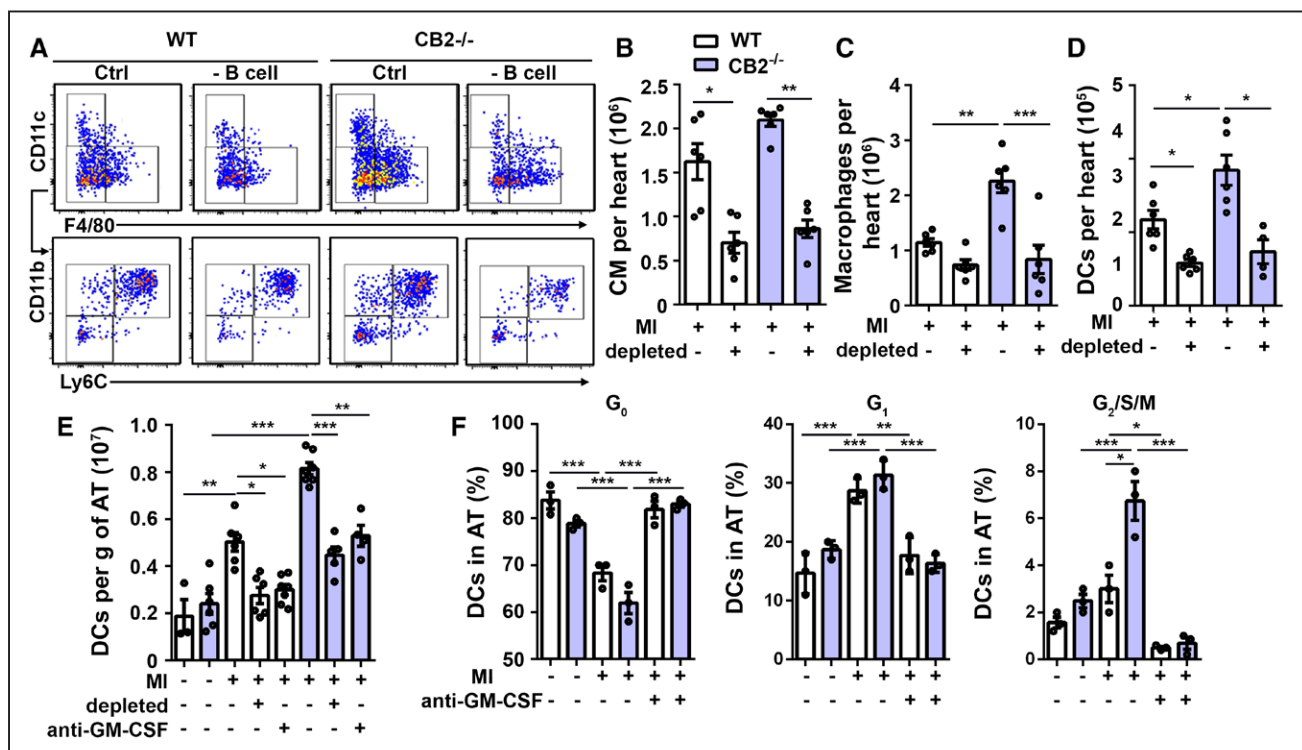


Figure 2. Myocardial infarction promotes accumulation of DCs in pericardial FALCs.

A, Gating strategy for flow-cytometric quantification of classical monocytes (CM) (**B**), macrophages (**C**), and DCs (**D**) detected in hearts of WT and CB2^{-/-} mice with or without B-cell depletion 3 days after MI (n=6). **E**, Quantification of DCs in pericardial AT of WT and CB2^{-/-} mice at steady state or 3 days after MI with or without B-cell depletion or GM-CSF blocking antibody, respectively. **F**, Percentage of resting and proliferating DCs in pericardial AT, at steady state or 3 days after MI with or without GM-CSF blocking antibody (n=3). Results are pooled from 3 independent experiments. Mean values±SEM are shown. *P<0.05. **P<0.01. ***P<0.001. AT indicates adipose tissue; Ctrl, control; DC, dendritic cell; FALC, fat-associated lymphoid cluster; G₀, cell cycle arrest; G₁, begin of cell cycle interphase; G₂, end of cell cycle interphase; GM-CSF, granulocyte-macrophage colony-stimulating factor; M, mitotic phase; MI, myocardial infarction; S, synthetic phase; and WT, wild type.

bution of DCs among lymphoid tissues revealed highest DC counts in spleens, without relevant differences 3 days after MI, whereas DCs significantly expanded in pericardial AT (Figure IVA in the online-only Data Supplement). A nonsignificant trend for DC expansion was also detected in draining lymph nodes after MI, but their numbers were much lower than in the pericardial AT.

GM-CSF plays an important role in the modulation of DC survival and proliferation.¹² We hypothesized that elevated levels of this cytokine released (among other cellular sources) by GM-CSF⁺ B cells in CB2^{-/-} mice were responsible for the massive DC expansion in these mice. Blocking of GM-CSF significantly reduced DC numbers in pericardial AT of both WT and CB2^{-/-} mice to levels comparable to the effects found after B-cell depletion (Figure 2E). Cell cycle analysis revealed that increased DC numbers in WT and CB2^{-/-} mice after MI were a consequence of enhanced proliferation, which was inhibited by GM-CSF blockade (Figure 2F). Conversely, splenectomy did not inhibit DC proliferation within pericardial AT, suggesting that splenic cells are not contributing to this effect (Figure IVB in the online-only Data Supplement).

DC Recruitment to Pericardial AT Requires CCR7

DCs are immune sentinels in peripheral tissues that, on antigen uptake, migrate to secondary lymphoid organs for the induction of immune responses.¹³ In support of DC trafficking during early inflammatory responses post-MI, we found massively increased circulating DC counts in CB2^{-/-} and, to a weaker extent, in WT mice 1 day after MI (Figure 3A). This was inhibited in part by B-cell depletion. To track DC migration from infarcted hearts to pericardial AT after MI, we injected fluorescently labeled immature DCs into infarcted hearts. We detected fluorescent DCs in pericardial AT 24 hours after cardiac injection, and some remaining fluorescent DCs in the infarct area, as well (Figure 3B), but no fluorescent signal within spleens (Figure IVC in the online-only Data Supplement).

DC maturation is reflected by expression of costimulatory molecules such as CD80 and CD86.¹⁴ We observed the lowest CD80 and CD86 expression levels in blood, intermediate levels in hearts, and highest levels in pericardial AT 3 days after MI (Figure 3C through 3E). Cardiac and pericardial AT expression levels of DC costimulatory molecules were higher in CB2^{-/-} than in WT mice 3 days post-MI, but lower in the case of B-cell depletion (Figure 3C through 3E).

CCR7 expressed by mature DCs¹⁵ is required for DC migration to lymphoid organs to initiate immune responses. We found an upregulation of CCR7 expression by cardiac and pericardial AT DCs after MI (Figure IVD in the online-only Data Supplement). In agreement with

the expression pattern of CD80 and CD86 maturation markers, we observed a mixed population of CCR7⁻ and CCR7⁺ DCs in the heart, whereas in AT, the major proportion of DCs after MI were CCR7⁺. CCL21, the ligand of CCR7, is constitutively released in secondary lymphoid organs and associated with the development of lymphoid structures in inflamed tissues. We found selective expression of this chemokine in pericardial but not subcutaneous AT of the same animals subjected to MI, with no difference between CB2^{-/-} and WT mice (Figure 3F and 3G).

To validate that DC migration to pericardial AT is mainly driven by the CCL21/CCR7 axis, we further investigated the impact of CCR7 deficiency on DC expansion in response to MI. Cardiac DC numbers were comparable in WT and CCR7^{-/-} mice 3 days after MI, whereas DC numbers in pericardial AT were significantly lower in CCR7^{-/-} mice (Figure 3H and 3I).

B Cells and GM-CSF Induce IL-17–Producing T Cells Within Pericardial AT

Mature DCs are specialized in activating T cells within lymphoid organs. Whole-mount 2-photon laser-scanning microscopy imaging indicated that CB2^{-/-} in comparison with WT mice displayed more T cells in FALCs at steady state and that MI induced a T-cell expansion (Figure 4A). Flow-cytometric quantification of T cells in pericardial AT confirmed higher counts in CB2^{-/-} than in WT mice at both steady state and after MI (Figure 4B). T-cell counts in mediastinal lymph nodes were much lower in comparison with pericardial AT, whereas most T cells are localized in the spleen (Figure VA in the online-only Data Supplement). However, pronounced T-cell expansion 3 days after MI was only detectable in pericardial AT, but not in spleen or lymph nodes. B-cell depletion or GM-CSF blockade, respectively, inhibited pericardial T-cell expansion in both WT and CB2^{-/-} mice (Figure 4B). CCR7^{-/-} mice subjected to MI did not show an expansion of T cells within pericardial AT (Figure 4B).

We further detected plasma cytokines produced by DCs and involved in lymphocyte polarization, ie, IL-1 α and IL-23, 24 hours after MI, with significantly higher plasma levels in CB2^{-/-} than in WT mice (Figure 4C). IL-23 induces IL-17 expression in T cells.¹⁶ We found significantly increased numbers of CD3⁺IL17⁺ cells within pericardial AT after MI, which were predominantly CD4-negative (Figure 4D and 4E) and expressed TCR $\gamma\delta$ (Figure VB in the online-only Data Supplement). Numbers of IL-17 expressing T cells were significantly higher in CB2^{-/-} than in WT mice (Figure 4D and 4E). The upregulation was inhibited by B-cell depletion or GM-CSF blockade in both genotypes. These findings were validated by gene expression analysis of pericardial AT and plasma cytokine levels of IL-17 (Figure 4F and 4G).

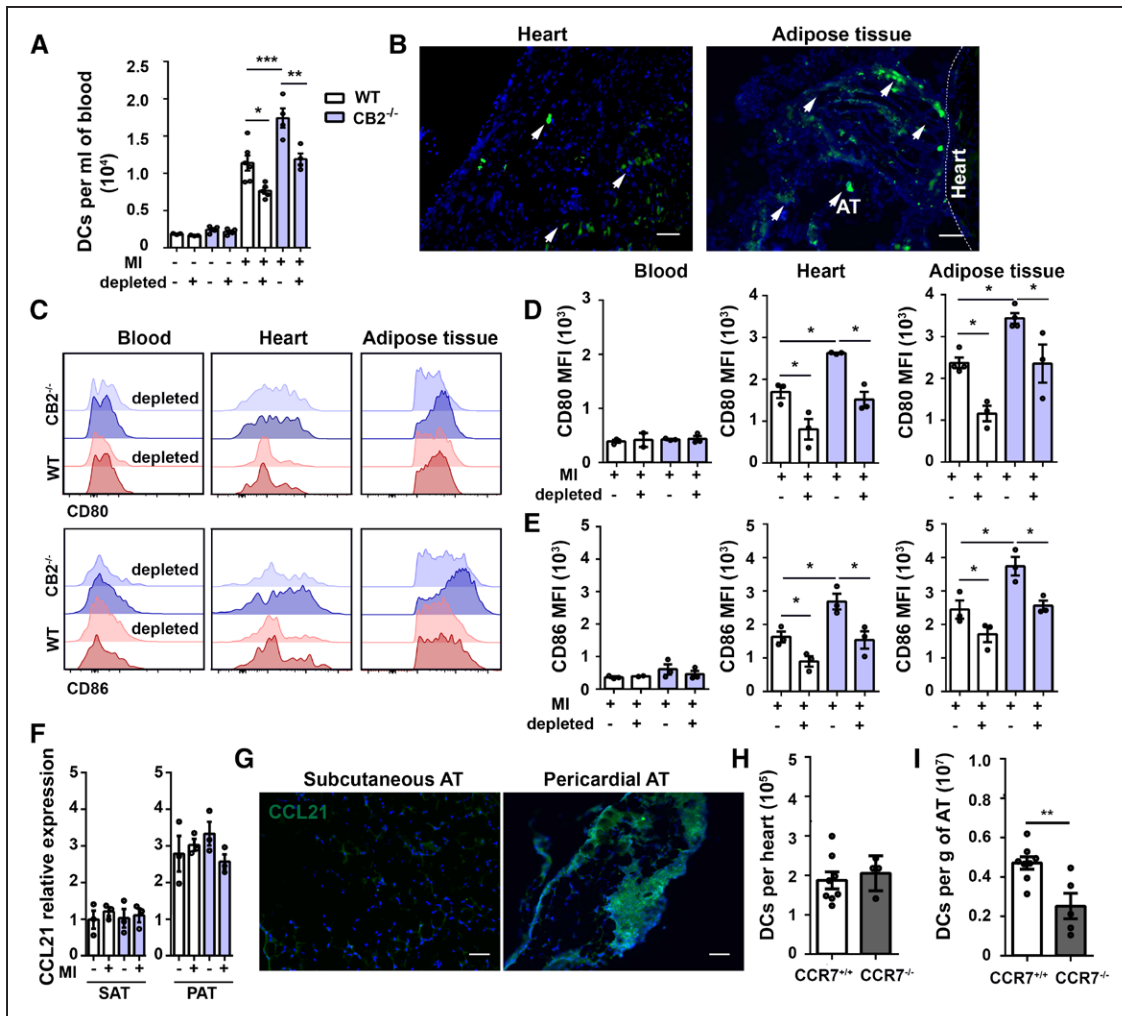


Figure 3. DCs are recruited to infarcted hearts and migrate to pericardial AT via CCR7.

A, Quantification of circulating DCs in blood of WT and $CB2^{-/-}$ mice with or without MI. **B**, Representative immunofluorescent images of DCs in infarcted heart and pericardial AT after intramyocardial injection of DCs labeled with cell tracker SP-DiOC18 (green) 24 hours after MI. Scale bars represent 50 μm . **C**, Representative histograms of maturation markers expressed by DCs in blood, heart, and pericardial AT of WT and $CB2^{-/-}$ mice subjected to MI with or without B-cell depletion (3 days after MI). Mean fluorescence intensities (MFI) of CD80 (**D**) and CD86 (**E**) staining on blood, heart, and pericardial AT DCs of WT and $CB2^{-/-}$ mice subjected to MI with or without B-cell depletion (3 days after MI). **F**, Quantification of CCL21 mRNA levels in pericardial AT (PAT), normalized to hypoxanthine guanine phospho ribosyltransferase, and represented as fold change in comparison with levels in subcutaneous AT (SAT) from WT and $CB2^{-/-}$ mice at steady state or 3 days after MI. **G**, Representative CCL21 immunostaining in SAT and PAT. The scale bar represents 50 μm . Flow-cytometric quantification of DCs in heart (**H**) and PAT (**I**) of $CCR7^{+/+}$ and $CCR7^{-/-}$ mice 3 days after MI. Results are pooled from 3 independent experiments ($n=3-6$). Mean values \pm SEM are shown. * $P<0.05$. ** $P<0.01$. *** $P<0.001$. AT indicates adipose tissue; DC, dendritic cell; MI, myocardial infarction; and WT, wild type.

MI-Induced Granulopoiesis and Second Wave of Cardiac Neutrophil Influx Is B-Cell Dependent

IL-17 signaling regulates granulocyte colony-stimulating factor (G-CSF) expression, which promotes granulopoiesis and neutrophil mobilization. G-CSF plasma levels post-MI were much higher in $CB2^{-/-}$ than in WT mice, but potently inhibited by B-cell depletion (Figure 5A). G-CSF can interact with other cytokines to induce hematopoiesis.¹⁷⁻¹⁹ Among cytokines produced by B cells,

we detected a significant upregulation of IL-3 and IL-6 in $CB2^{-/-}$ in comparison with WT mice 24 hours after MI (Figure VIA in the online-only Data Supplement). In support of enhanced bone marrow activation, flow cytometry and whole-mount 2-photon laser-scanning microscopy imaging confirmed higher numbers of hematopoietic stem and progenitor cells in $CB2^{-/-}$ than in WT mice, both at steady state and after MI (Figure 5B through 5D and Figure VIB in the online-only Data Supplement). Cell cycle analysis confirmed that this increase was attributable to enhanced proliferation of

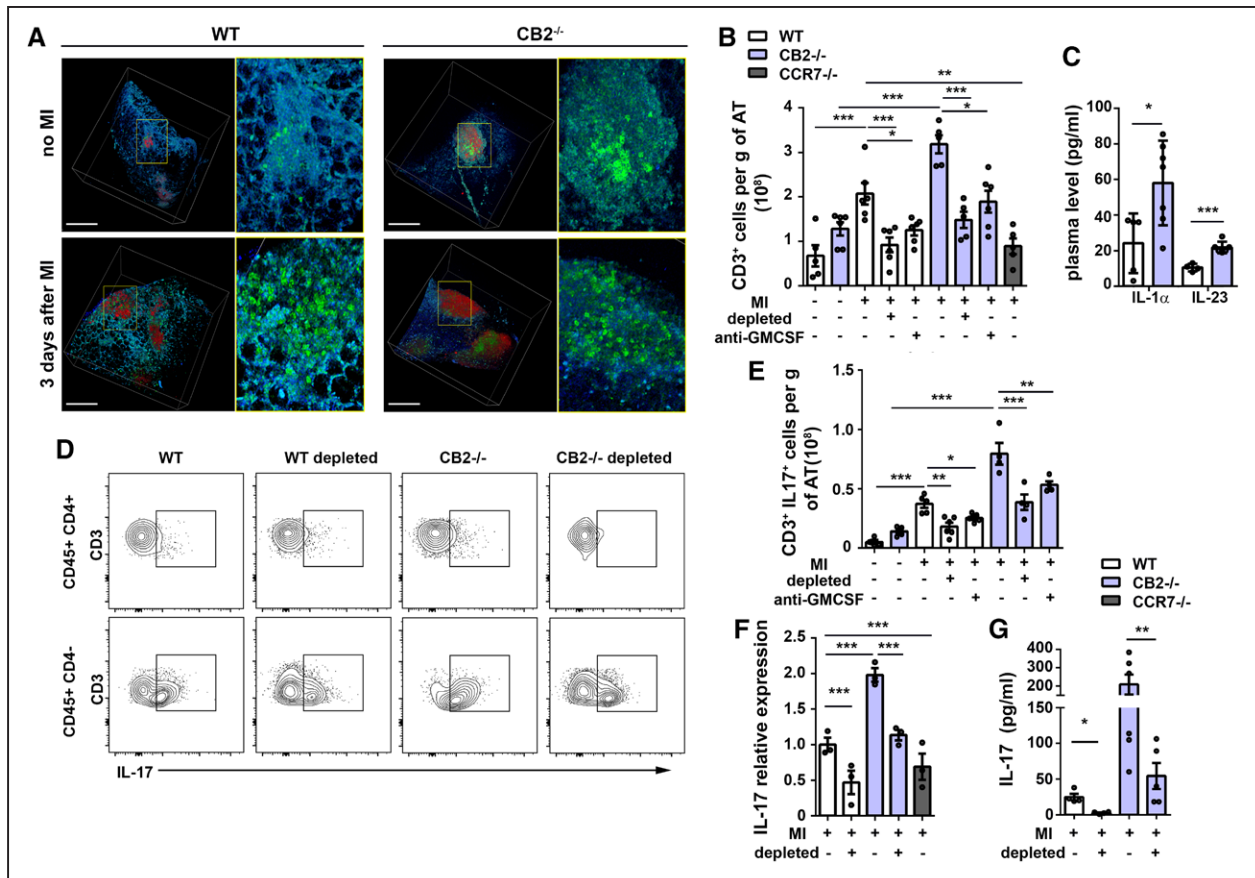


Figure 4. MI promotes accumulation of IL-17⁺ T cells in pericardial AT.

A, Three-dimensional TPLSM reconstruction of CD19⁺ B cells (red), CD3⁺ T cells (green), and autofluorescent components (collagen, adipocytes; blue) in pericardial AT of WT and CB2^{-/-} mice. Higher magnification of T-cell clusters are shown without B cells. Scale bars represent 200 μ m. **B**, Flow-cytometric quantification of T cells in pericardial AT of WT, CB2^{-/-}, and CCR7^{-/-} mice at baseline or subjected to MI, B-cell depletion, or injection of GM-CSF–blocking antibody as indicated (3 days after MI). **C**, Plasma cytokine levels 24 hours after MI. **D**, Gating strategy used for the quantification of T-lymphocyte populations in pericardial AT. **E**, Number of IL-17⁺ T cells in pericardial AT of WT and CB2^{-/-} mice at baseline or subjected to MI, B-cell depletion, or injection of GM-CSF–blocking antibody as indicated (3 days after MI). **F**, IL-17 mRNA expression levels in pericardial AT 3 days after MI with or without B-cell depletion in WT, CB2^{-/-}, and CCR7^{-/-} mice, normalized to hypoxanthine guanine phospho ribosyltransferase and represented as fold change in comparison with WT mice with MI. **G**, Plasma levels of IL-17, 24 hours after MI with or without B-cell depletion in WT and CB2^{-/-} mice. Results are pooled from 3 independent experiments (n=3–7). Mean values \pm SEM are shown. **P*<0.05. ***P*<0.01. ****P*<0.001. AT indicates adipose tissue; GM-CSF, granulocyte-macrophage colony-stimulating factor; IL, interleukin; MI, myocardial infarction; TPLSM, 2-photon laser-scanning microscopy; and WT, wild type.

hematopoietic stem cells, multipotent progenitors, and hematopoietic progenitors (Figure 5E). B-cell depletion resulted in reduced numbers of lineage-negative, Sca1-positive, c-kit–positive cells, confirming a crucial role for B cells in regulating hematopoiesis post-MI (Figure 5F).

In support of enhanced granulopoiesis, CB2^{-/-} mice had higher granulocyte-macrophage progenitor (GMP) numbers in response to MI in comparison with WT mice, whereas B-cell depletion significantly decreased MI-induced increase in GMP numbers (Figure 5G and Figure VIC in the online-only Data Supplement). GMP counts were much lower in CCR7^{-/-} mice. We further assessed the effect of CB2 deficiency or B-cell depletion, respectively, on cardiac neutrophil infiltration post-

MI. B-cell depletion did not affect early neutrophil infiltration within 24 hours (Figure 5H), suggesting that a large reservoir of bone marrow neutrophils is readily released after MI. Three days post-MI, cardiac neutrophil counts were significantly lower after B-cell depletion, GM-CSF blockade, or CCR7 deficiency, suggesting an inhibition of emergency granulopoiesis.

Pericardial Adipose Tissue Controls MI-Induced Granulopoiesis

Because pericardial AT is not the only source for B cells and GM-CSF production, we aimed to clarify the specific contribution of pericardial AT in promoting granulopoi-

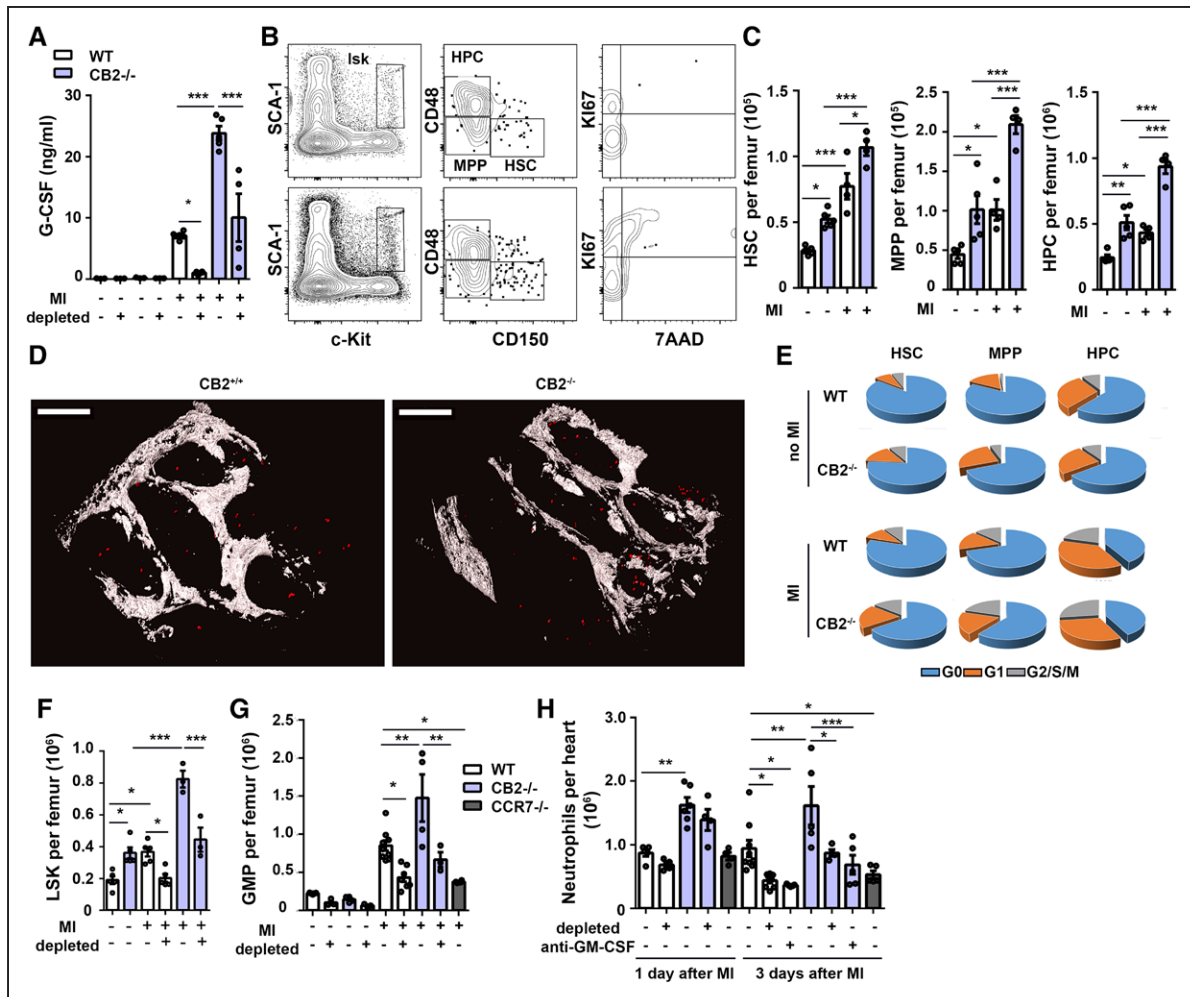


Figure 5. B cells promote emergency granulopoiesis after MI.

A, G-CSF plasma levels of WT and CB2^{-/-} mice at steady state or 1 day after MI with or without B-cell depletion. **B**, Plots represent the gating strategy used for flow-cytometric quantification of resting and proliferating bone marrow stem cell populations of WT (upper dot plots) and CB2^{-/-} mice (lower dot plots). **C**, Quantification of hematopoietic stem cells (HSC), multipotent progenitor (MPP), and hematopoietic progenitor cells (HPC) in femurs of WT and CB2^{-/-} mice at steady state or 1 day after MI with or without B-cell depletion. **D**, TPLSM reconstruction of CD150⁺ HSCs (red) after exclusion of Lin (CD3, CD11b, B220, Gr-1, Ter119, CD41) and CD48 in bone marrow (femoral metaphysis) of WT and CB2^{-/-} mice 1 day after MI. Scale bars represent 150 μm. **E**, Relative distribution of HSC, MPP, and HPC within the bone marrow in the different cell cycle phases, before and 1 day after MI, determined by flow cytometry. **F**, Flow-cytometric quantification of lineage-negative, Sca1-positive, c-kit-positive (LSK) in WT and CB2^{-/-} mice at steady state or 1 day after MI with or without B-cell depletion. **G**, Quantification of GMP in WT, CB2^{-/-}, and CCR7^{-/-} mice at steady state or 1 day after MI with or without B-cell depletion. **H**, Quantification of neutrophils in digested hearts of WT, CB2^{-/-}, and CCR7^{-/-} mice, at steady state, 1 or 3 days after MI with or without B-cell depletion or injected with GM-CSF-blocking antibody. Results are pooled from 3 independent experiments (n=3–9). Mean values±SEM are shown. *P<0.05. **P<0.01. ***P<0.001. G0 indicates cell cycle arrest; G1, begin of cell cycle interphase; G2, end of cell cycle interphase; M, mitotic phase; MI, myocardial infarction; S, synthetic phase; TPLSM, 2-photon laser-scanning microscopy; and WT, wild type.

esis in response to MI. For this purpose, we first performed an ex vivo coculture experiment. MI was induced in WT mice, and the pericardial AT was removed 3 days later and subsequently exposed to freshly isolated bone marrow cells. The coculture resulted in a massive expansion of GMPs, whereas pericardial AT from noninfarcted mice did not markedly increase GMP counts (Figure 6A). No mitogenic effects were observed when coculturing bone marrow cells with subcutaneous AT from the same

mice. Likewise, exposure of progenitors to adipocyte-conditioned medium did not induce proliferation (Figure 6A), suggesting that immune cells within pericardial AT, rather than adipocytes, promote GMP proliferation.

To provide in vivo evidence that the pericardial AT is involved in the regulation of granulopoiesis in response to MI, we surgically removed the pericardial AT when subjecting mice to LAD ligation. The analysis 3 days after MI revealed a 50% reduction of GMP counts in the

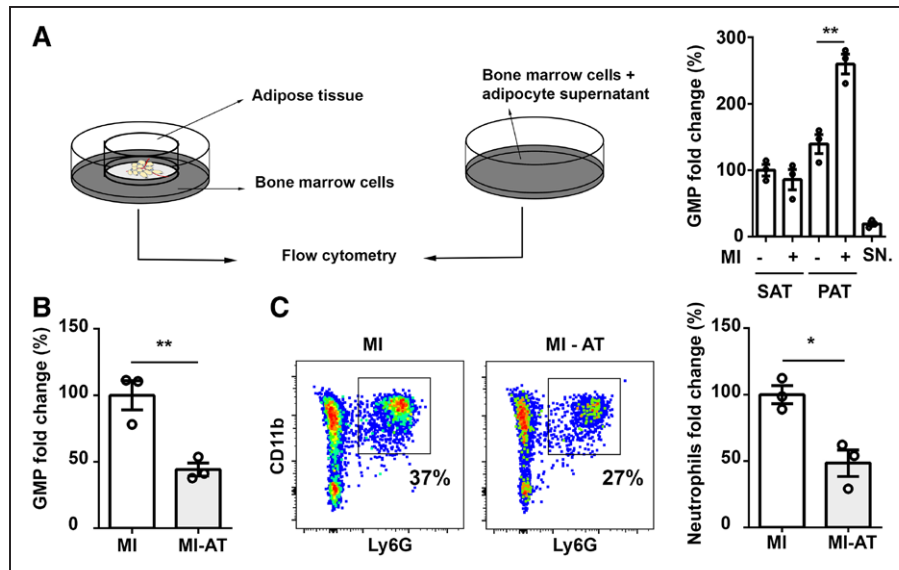


Figure 6. Pericardial adipose tissue regulates granulopoiesis after MI.

A, WT bone marrow cells were cocultured with subcutaneous (SAT) or pericardial adipose tissue (PAT) or treated with adipocyte culture supernatant (SN). AT for coculture and isolation of adipocytes was isolated from WT mice 3 days after MI or mice without MI. GMP counts were quantified by flow cytometry after 48 hours of stimulation. **B** and **C**, Effect of surgical removal of pericardial AT before LAD ligation (MI-AT) on GMP expansion in the bone marrow (**B**) and neutrophil recruitment to the myocardium (**C**) 3 days after MI in WT mice. Data are expressed relative to infarcted mice without AT removal (MI, defined as 100%). Mean values \pm SEM are shown. * P <0.05. ** P <0.01. AT indicates adipose tissue; GMP, granulocyte-macrophage progenitor; LAD, left anterior descending coronary artery; MI, myocardial infarction; and WT, wild type.

bone marrow (Figure 6B) and a comparable reduction of neutrophils in the myocardium (Figure 6C).

B Cells and Pericardial AT Regulate Fibrosis and Cardiac Function Post-MI

Finally, to address the structural and functional consequences of enhanced B-cell activation in pericardial AT, we performed histochemical analysis of hearts 7 days post-MI, which is the fibrotic phase succeeding the resolved inflammatory phase. Masson trichrome staining revealed a significantly higher content of left ventricular fibrosis in infarcted hearts of $CB2^{-/-}$ in comparison with WT mice (Figure 7A and 7B). This massive increase of fibrosis was inhibited by B-cell depletion or surgical removal of pericardial AT. In line with larger fibrotic scar formation, $CB2^{-/-}$ mice had a significantly more impaired left ventricular function 7 days after MI than WT mice, reflected by a higher reduction in ejection fraction between sham and infarcted mice (Figure 7C). This more pronounced loss of left ventricular function in $CB2^{-/-}$ mice was prevented by either B-cell depletion or surgical removal of pericardial AT (Figure 7C).

DISCUSSION

The murine pericardial AT contains a high density of lymphoid clusters, suggesting that they might play a relevant role in regulating cardiac homeostasis. Here,

we have identified a new function for pericardial AT in promoting granulopoiesis induced by ischemic cardiac injury. The quantity of B cells, DCs, and T cells in murine pericardial AT largely exceeds their numbers in the myocardium. Although GM-CSF-producing B cells are produced and stored in the spleen¹¹ during homeostasis, they preferentially expand in the pericardial AT in response to ischemic cardiac injury. Similarly, MI-induced DC and T-cell expansion occurs in pericardial AT, with numerically lower increases in heart-draining lymph nodes. It is remarkable that this expansion was not observed in other AT beds, suggesting a specific mechanism in the pericardial AT after MI.

Previous studies addressing the role of lymphocytes and DCs in MI mainly focused on their local presence in the myocardium and long-term effects on cardiac remodeling. However, their cardiac numbers are relatively low and peak around day 7 after MI in murine models of permanent ligation.^{1,20–22} Similarly, B cells have been detected in infarcted myocardium, peaking at day 5 post-MI.¹ Release of CCL7 in response to MI and consequently monocyte mobilization has been attributed to splenic B cells.¹ B cells are heterogeneous subsets with distinct immunologic functions. Mature B2 cells depend on B-cell activating factor receptor signaling.²³ Genetic B-cell activating factor receptor deficiency or antibody-mediated blockade of CD20 or B-cell activating factor, which preferentially depletes B2 cells, limits cardiac fibrosis, and improves cardiac function parame-

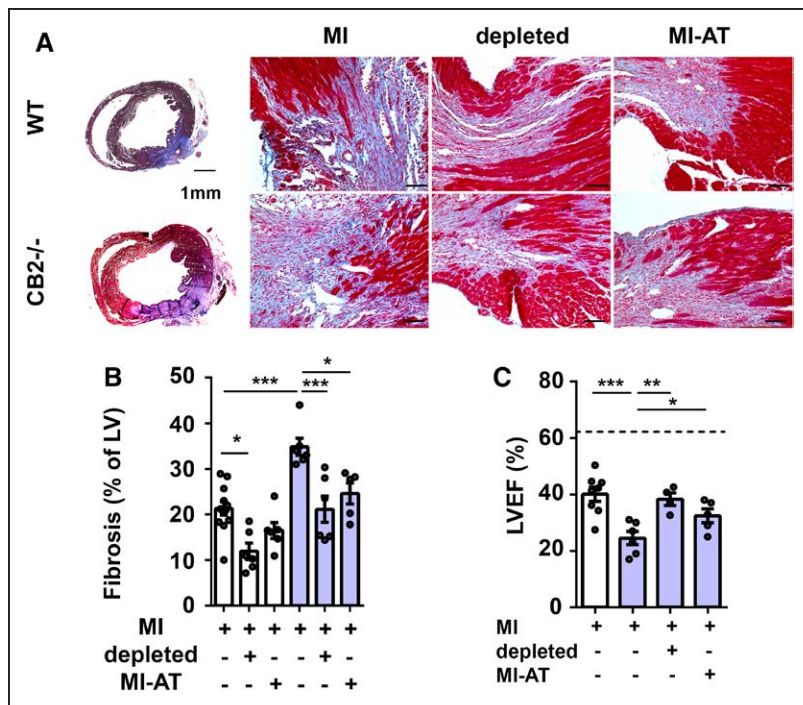


Figure 7. Pericardial adipose tissue regulates MI outcome.

A, Representative images of WT and CB2^{-/-} mice 7 days after MI stained with Masson trichrome (collagen, blue). Whole heart cross-sections (2.5× magnification, **Left**) and border zone (20× magnification, **Right**, scale bar represents 50 μm) are shown. **B**, Quantification of collagen in WT and CB2^{-/-} hearts 7 days after MI with or without B-cell depletion (depleted) or surgical removal of pericardial AT (MI-AT; n=6 per group). **C**, Echocardiographic assessment of left ventricular ejection fraction (LVEF) in WT or CB2^{-/-} mice with or without B-cell depletion or surgical removal of pericardial AT, 7 days after MI (n=4–7). The dotted line corresponds to the WT sham group. Mean values±SEM are shown. *P<0.05. **P<0.01. ***P<0.001. AT indicates adipose tissue; LV, left ventricle; LVEF, left ventricular ejection fraction; MI, myocardial infarction; and WT, wild type.

ters 14 days after MI. A distinct subset, more related to B1 cells, is innate response activator B cells that develop in the spleen and have been described in the peritoneal and pleural cavity during sepsis and pneumonia.^{11,24} Innate response activator B cells secrete GM-CSF, which regulates, among other functions, DC physiology¹² and is required for IL-23 secretion by DCs and IL-17-producing T cells.²⁵ IL-17 released by $\gamma\delta$ T cells controls granulopoiesis through G-CSF.²⁶ The relevance of the IL-23/IL-17 axis in MI healing responses has been previously demonstrated in experimental studies.^{16,27} B cells are not required for early neutrophil mobilization within the first 24 hours after MI, because B-cell depletion did not inhibit early neutrophil infiltration. The bone marrow serves as a reservoir in which >90% of neutrophils are stored at steady state. After ischemic cardiac injury, bone marrow stromal cells respond by releasing G-CSF, which induces rapid de novo neutrophil production referred to as emergency granulopoiesis.²⁸ Concomitant with GMP expansion, we observed a strong reduction of lymphopoietic progenitors 24 hours after MI, reflecting the shift toward enhanced granulopoiesis. In support of a role for B cells and GM-CSF release in promoting granulopoiesis after MI, B-cell depletion or GM-CSF blockade inhibited granulopoiesis and a second wave of cardiac neutrophil infiltration. We further confirmed the pericardial AT as a major source for factors regulating emergency granulopoiesis after MI. Our in vitro findings suggest that factors released by adipocytes alone are not involved in this regulation.

We used the CB2^{-/-} mice as strategy to assess the effects of enhanced B-cell activation on post-MI inflammatory responses. We found that the cannabinoid

receptor CB2 regulates B-cell and GM-CSF⁺ B-cell expansion within pericardial AT. CB2 is required for the retention of immature B cells within the bone marrow sinusoidal niche¹⁰ and positioning of marginal zone B cells in the spleen.²⁹ Because bone marrow lymphopoiesis is not affected by CB2 deficiency, higher B-cell counts in CB2^{-/-} hearts and pericardial AT are rather a consequence of impaired bone marrow retention and enhanced activation. All relevant cytokines involved in B-cell, DC, and T-cell activation are systemically elevated in CB2^{-/-} mice after MI. Enhanced GM-CSF/IL-17/G-CSF signaling in CB2^{-/-} mice translates into more pronounced emergency granulopoiesis and higher cardiac neutrophil infiltration post-MI. Our B-cell depletion and GM-CSF-blocking experiments in CB2^{-/-} mice indicate that this effect depends on early B-cell activation and GM-CSF release, which subsequently enhances DC and T-cell expansion, and granulopoiesis, as well. Although a certain amount of neutrophils is required for regulated cardiac healing and priming of reparative macrophages that remove cell debris in the infarct area,³⁰ excessive cardiac neutrophil influx may promote an unfavorable remodeling process.³¹ In line with a detrimental effect of enhanced cardiac neutrophil infiltration attributable to upregulated granulopoiesis, infarcted CB2^{-/-} mice had a more reduced ejection fraction than infarcted WT mice. The histological and functional data are in agreement with previous studies reporting unfavorable MI healing in the absence of CB2.^{32,33} Our novel finding that left ventricular fibrosis and cardiac function decline was less pronounced after B-cell depletion or removal of pericardial AT highlights the major role of pericardial AT and B cells in the modulation of post-MI outcome.

A limitation of our experimental approach based on systemic B-cell depletion is that the observed effects might not be solely a consequence of impaired B-cell activation in the pericardial AT. Another limitation is that CB2 is expressed by different leukocyte populations and nonhematopoietic cells, whereas we only used conventional CB2^{-/-} mice in this study. To strengthen the conclusions that can be drawn from our study, we have used a combination of mouse models and strategies in WT and CB2^{-/-} mice (B-cell depletion, GM-CSF blockade, and pericardial AT removal). Thereby, we could validate a novel mechanism driven by pericardial AT B cells that coordinates early inflammatory responses post-MI. This might have potential relevance for human pathophysiology, as suggested by the presence of B-cell-rich clusters in human epicardial AT of patients with CAD. Moreover, analysis of human transcortical gradients, obtained from patients with MI during revascularization intervention to reopen the occluded coronary artery, hints to an early recruitment of lymphocytes into the myocardium or possibly epicardial AT.²

Nevertheless, some open questions still remain that deserve further investigation, such as the local milieu promoting B- and T-cell expansion in AT. We may speculate that there is a specific cross-talk between adipocytes and lymphocytes, which raises the question whether metabolic changes and chronic AT inflammation in obese patients affects B-cell function and pericardial AT immune cell activation in the setting of an acute MI. As to the local differences that may promote specific recruitment to lymphoid clusters within pericardial AT, we found that the secondary lymphoid tissue chemokine CCL21 is specifically expressed in pericardial but not subcutaneous AT. Upregulation of CCR7 on mature DCs might thereby support their homing from their site of activation in the infarcted myocardium to lymphoid clusters present in pericardial AT. Finally, activation of pericardial lymphoid clusters in response to MI might have additional effects beyond stimulation of granulopoiesis, which could also affect cardiac healing. Unveiling the specific function of pericardial GM-CSF⁺ B-cell expansion on cardiac outcome will require further studies based on genetic models selectively depleting GM-CSF-producing B cells.

In conclusion, we have identified the pericardial AT as an immunologically active organ in which lymphocyte subsets contribute to rapid immune responses. A better knowledge of its complex regulation under homeostatic and pathophysiological conditions might further enhance our understanding of cardiac stress responses to severe events such as an acute MI. This might eventually lead to new approaches for more targeted and better balanced inflammatory therapies to improve MI outcome.

ARTICLE INFORMATION

Received April 7, 2017; accepted November 1, 2017.

The online-only Data Supplement is available with this article at <http://circ.ahajournals.org/lookup/suppl/doi:10.1161/CIRCULATIONAHA.117.028833/-DC1>.

Correspondence

Sabine Steffens, PhD, Institute for Cardiovascular Prevention, Pettenkoferstr 9, 80336 Munich, Germany. E-mail sabine.steffens@med.uni-muenchen.de

Affiliations

Institute for Cardiovascular Prevention, Ludwig-Maximilians-University, Munich, Germany (M.B., D.S., R.T.A.M., C.W., J.D., S.S.). Institut de Recherche Interdisciplinaire en Biologie Humaine et Moléculaire, Université Libre de Bruxelles (U.L.B.), Brussels, Belgium (M.H., J.-Y.S., I.N.). Department of Biomedical Engineering (R.T.A.M.), and Department of Biochemistry (C.W.), Cardiovascular Research Institute Maastricht, Maastricht University, Netherlands. Department of Interdisciplinary Medicine (M.V.), Clinica Medica "C. Frugoni," (A.M.), University of Bari "Aldo Moro," Italy. Ageing Research Center, "G. d'Annunzio" University Foundation, Chieti, Italy (M.V.). University of Cambridge, United Kingdom (M.V.). Cardiovascular Department, "S.Orsola Malpighi" Hospital, University of Bologna, Italy (M.D.E.). Cardiac Surgery Unit, Ospedali Riuniti of Ancona, Italy (M.D.E.). Cardiac Surgery Department, Ospedali Riuniti "Umberto I-Lancisi-Salesi," Ancona, Italy (M.D.E.). German Center for Cardiovascular Research, partner site Munich Heart Alliance, Germany (C.W., S.S.).

Acknowledgments

Dr Horckmans performed all surgical procedures, echocardiography recordings, flow cytometry, histology, gene expression analysis, immunologic assays, and analyzed data. Mrs Negri performed some murine adipose tissue analyses. Mrs Bianchini and Dr Megens performed 2-photon laser-scanning microscopy. Drs Horckmans and Santovito performed statistical analyses. Dr Springael provided CCR7-deficient mice. Drs Vacca, Di Eusanio, and Moschetta generated a human biobank and provided human adipose tissue samples. Dr Weber provided substantial funding and critical input for the study design. Drs Horckmans, Duchene, and Steffens designed the study and wrote the manuscript. All authors discussed results and commented on the manuscript. CB2^{-/-} mice were kindly provided by Andreas Zimmer, Bonn, Germany.

Sources of Funding

This work was supported in part by the Deutsche Forschungsgemeinschaft (STE-1053/3-1 and STE-1053/5-1 to Dr Steffens, SFB1123 TP A1 to Dr Weber, Z1 to Dr Megens, and INST409/97-1 to Drs Weber and Megens), Innoviris (Attract-Brains for Brussels to Dr Horckmans), and the European Research Council (ERC AdG 249929 to Dr Weber).

Disclosures

None.

REFERENCES

- Zougari Y, Ait-Oufella H, Bonnin P, Simon T, Sage AP, Guérin C, Vilar J, Caligiuri G, Tsiantoulas D, Laurans L, Dumeau E, Kotti S, Bruneval P, Charo IF, Binder CJ, Danchin N, Tedgui A, Tedder TF, Silvestre JS, Mallat Z. B lymphocytes trigger monocyte mobilization and impair heart function after acute myocardial infarction. *Nat Med*. 2013;19:1273–1280. doi: 10.1038/nm.3284.
- Boag SE, Das R, Shmeleva EV, Bagnall A, Egred M, Howard N, Bennaceur K, Zaman A, Keavney B, Spyridopoulos I. T lymphocytes and fractalkine contribute to myocardial ischemia/reperfusion injury in patients. *J Clin Invest*. 2015;125:3063–3076. doi: 10.1172/JCI80055.
- Iacobellis G, Corradi D, Sharma AM. Epicardial adipose tissue: anatomic, biomolecular and clinical relationships with the heart. *Nat Clin Pract Cardiovasc Med*. 2005;2:536–543. doi: 10.1038/ncpcardio0319.

4. Bénézech C, Luu NT, Walker JA, Kruglov AA, Loo Y, Nakamura K, Zhang Y, Nayar S, Jones LH, Flores-Langarica A, McIntosh A, Marshall J, Barone F, Besra G, Miles K, Allen JE, Gray M, Kollias G, Cunningham AF, Withers DR, Toellner KM, Jones ND, Veldhoen M, Nedospasov SA, McKenzie ANJ, Caamaño JH. Inflammation-induced formation of fat-associated lymphoid clusters. *Nat Immunol*. 2015;16:819–828. doi: 10.1038/ni.3215.
5. Buckley NE, McCoy KL, Mezey E, Bonner T, Zimmer A, Felder CC, Glass M, Zimmer A. Immunomodulation by cannabinoids is absent in mice deficient for the cannabinoid CB(2) receptor. *Eur J Pharmacol*. 2000;396:141–149.
6. Schneider MA, Meingassner JG, Lipp M, Moore HD, Rot A. CCR7 is required for the *in vivo* function of CD4+ CD25+ regulatory T cells. *J Exp Med*. 2007;204:735–745. doi: 10.1084/jem.20061405.
7. Keren Z, Naor S, Nussbaum S, Golan K, Itkin T, Sasaki Y, Schmidt-Supprian M, Lapidot T, Melamed D. B-cell depletion reactivates B lymphopoiesis in the BM and rejuvenates the B lineage in aging. *Blood*. 2011;117:3104–3112. doi: 10.1182/blood-2010-09-307983.
8. Kulcsar KA, Baxter VK, Greene IP, Griffin DE. Interleukin 10 modulation of pathogenic Th17 cells during fatal alphavirus encephalomyelitis. *Proc Natl Acad Sci USA*. 2014;111:16053–16058. doi: 10.1073/pnas.1418966111.
9. Pacher P, Mechoulam R. Is lipid signaling through cannabinoid 2 receptors part of a protective system? *Prog Lipid Res*. 2011;50:193–211. doi: 10.1016/j.plipres.2011.01.001.
10. Pereira JP, An J, Xu Y, Huang Y, Cyster JG. Cannabinoid receptor 2 mediates the retention of immature B cells in bone marrow sinusoids. *Nat Immunol*. 2009;10:403–411. doi: 10.1038/ni.1710.
11. Rauch PJ, Chudnovskiy A, Robbins CS, Weber GF, Eitzrodt M, Hilgendorf I, Tiglaio E, Figueiredo JL, Iwamoto Y, Theurl I, Gorbatov R, Waring MT, Chicoine AT, Mouded M, Pittet MJ, Nahrendorf M, Weissleder R, Swirski FK. Innate response activator B cells protect against microbial sepsis. *Science*. 2012;335:597–601. doi: 10.1126/science.1215173.
12. van de Laar L, Coffey PJ, Woltman AM. Regulation of dendritic cell development by GM-CSF: molecular control and implications for immune homeostasis and therapy. *Blood*. 2012;119:3383–3393.
13. Mildner A, Jung S. Development and function of dendritic cell subsets. *Immunity*. 2014;40:642–656. doi: 10.1016/j.immuni.2014.04.016.
14. Banchereau J, Briere F, Caux C, Davoust J, Lebecque S, Liu YJ, Pulendran B, Palucka K. Immunobiology of dendritic cells. *Annu Rev Immunol*. 2000;18:767–811. doi: 10.1146/annurev.immunol.18.1.767.
15. Sallusto F, Palermo B, Lenig D, Miettinen M, Matikainen S, Julkunen I, Forster R, Burgstahler R, Lipp M, Lanzavecchia A. Distinct patterns and kinetics of chemokine production regulate dendritic cell function. *Eur J Immunol*. 1999;29:1617–1625. doi: 10.1002/(SICI)1521-4141(199905)29:05<1617::AID-IMMU1617>3.0.CO;2-3.
16. Yan X, Shichita T, Katsumata Y, Matsuhashi T, Ito H, Ito K, Anzai A, Endo J, Tamura Y, Kimura K, Fujita J, Shinmura K, Shen W, Yoshimura A, Fukuda K, Sano M. Deleterious effect of the IL-23/IL-17A axis and $\gamma\delta$ T cells on left ventricular remodeling after myocardial infarction. *J Am Heart Assoc*. 2012;1:e004408. doi: 10.1161/JAHA.112.004408.
17. Moore MA, Warren DJ. Synergy of interleukin 1 and granulocyte colony-stimulating factor: *in vivo* stimulation of stem-cell recovery and hematopoietic regeneration following 5-fluorouracil treatment of mice. *Proc Natl Acad Sci USA*. 1987;84:7134–7138.
18. Pojda Z, Tanaka K, Aoki Y, Tsuboi A. *In vivo* and *in vitro* interaction between interleukin 6 and granulocyte colony-stimulating factor in the regulation of murine hematopoiesis. *Exp Hematol*. 1992;20:874–878.
19. McNiece I, Andrews R, Stewart M, Clark S, Boone T, Quesenberry P. Action of interleukin-3, G-CSF, and GM-CSF on highly enriched human hematopoietic progenitor cells: synergistic interaction of GM-CSF plus G-CSF. *Blood*. 1989;74:110–114.
20. Yan X, Anzai A, Katsumata Y, Matsuhashi T, Ito K, Endo J, Yamamoto T, Takeshima A, Shinmura K, Shen W, Fukuda K, Sano M. Temporal dynamics of cardiac immune cell accumulation following acute myocardial infarction. *J Mol Cell Cardiol*. 2013;62:24–35. doi: 10.1016/j.yjmcc.2013.04.023.
21. Anzai A, Anzai T, Nagai S, Maekawa Y, Naito K, Kaneko H, Sugano Y, Takahashi T, Abe H, Mochizuki S, Sano M, Yoshikawa T, Okada Y, Koyasu S, Ogawa S, Fukuda K. Regulatory role of dendritic cells in postinfarction healing and left ventricular remodeling. *Circulation*. 2012;125:1234–1245. doi: 10.1161/CIRCULATIONAHA.111.052126.
22. Hofmann U, Beyersdorf N, Weirather J, Podolskaya A, Bauersachs J, Ertl G, Kerkau T, Frantz S. Activation of CD4+ T lymphocytes improves wound healing and survival after experimental myocardial infarction in mice. *Circulation*. 2012;125:1652–1663. doi: 10.1161/CIRCULATIONAHA.111.044164.
23. Tsiantoulas D, Sage AP, Mallat Z, Binder CJ. Targeting B cells in atherosclerosis: closing the gap from bench to bedside. *Arterioscler Thromb Vasc Biol*. 2015;35:296–302. doi: 10.1161/ATVBAHA.114.303569.
24. Weber GF, Chousterman BG, Hilgendorf I, Robbins CS, Theurl I, Gerhardt LM, Iwamoto Y, Quach TD, Ali M, Chen JW, Rothstein TL, Nahrendorf M, Weissleder R, Swirski FK. Pleural innate response activator B cells protect against pneumonia via a GM-CSF-IgM axis. *J Exp Med*. 2014;211:1243–1256. doi: 10.1084/jem.20131471.
25. McGeachy MJ. GM-CSF: the secret weapon in the T(H)17 arsenal. *Nat Immunol*. 2011;12:521–522. doi: 10.1038/ni.2044.
26. Stark MA, Huo Y, Burcin TL, Morris MA, Olson TS, Ley K. Phagocytosis of apoptotic neutrophils regulates granulopoiesis via IL-23 and IL-17. *Immunity*. 2005;22:285–294. doi: 10.1016/j.immuni.2005.01.011.
27. Barry SP, Ounzain S, McCormick J, Scarabelli TM, Chen-Scarabelli C, Saravolatz LI, Faggian G, Mazzucco A, Suzuki H, Thiemeermann C, Knight RA, Latchman DS, Stephanou A. Enhanced IL-17 signalling following myocardial ischaemia/reperfusion injury. *Int J Cardiol*. 2013;163:326–334. doi: 10.1016/j.ijcard.2011.08.849.
28. Manz MG, Boettcher S. Emergency granulopoiesis. *Nat Rev Immunol*. 2014;14:302–314. doi: 10.1038/nri3660.
29. Muppidi JR, Arnon TI, Bronevetsky Y, Veerapen N, Tanaka M, Besra GS, Cyster JG. Cannabinoid receptor 2 positions and retains marginal zone B cells within the splenic marginal zone. *J Exp Med*. 2011;208:1941–1948. doi: 10.1084/jem.20111083.
30. Horckmans M, Ring L, Duchene J, Santovito D, Schloss MJ, Drechsler M, Weber C, Soehnlein O, Steffens S. Neutrophils orchestrate post-myocardial infarction healing by polarizing macrophages towards a reparative phenotype. *Eur Heart J*. 2017;38:187–197. doi: 10.1093/eurheartj/ehw002.
31. Schloss MJ, Horckmans M, Nitz K, Duchene J, Drechsler M, Bidzhekov K, Scheiermann C, Weber C, Soehnlein O, Steffens S. The time-of-day of myocardial infarction onset affects healing through oscillations in cardiac neutrophil recruitment. *EMBO Mol Med*. 2016;8:937–948. doi: 10.15252/emmm.201506083.
32. Defer N, Wan J, Souktani R, Escoubet B, Perier M, Caramelle P, Manin S, Deveaux V, Bourin MC, Zimmer A, Lotersztajn S, Pecker F, Pavoine C. The cannabinoid receptor type 2 promotes cardiac myocyte and fibroblast survival and protects against ischemia/reperfusion-induced cardiomyopathy. *FASEB J*. 2009;23:2120–2130. doi: 10.1096/fj.09-129478.
33. Duerr GD, Heinemann JC, Suchan G, Kolobara E, Wenzel D, Geisen C, Matthey M, Pässe-Tietjen K, Mahmud W, Ghanem A, Tiemann K, Alferink J, Burgdorf S, Buchalla R, Zimmer A, Lutz B, Welz A, Fleischmann BK, Dewald O. The endocannabinoid-CB2 receptor axis protects the ischemic heart at the early stage of cardiomyopathy. *Basic Res Cardiol*. 2014;109:425. doi: 10.1007/s00395-014-0425-x.